JOURNAL OF VIROLOGY, Aug. 2008, p. 7284–7297 Vol. 82, No. 15
0022-538X/08/$08.00+0 doi:10.1128/JVI.00224-08

Role for Conserved Residues of Sindbis Virus Nonstructural Protein 2 Methyltransferase-Like Domain in Regulation of Minus-Strand Synthesis and Development of Cytopathic Infection▽†

Mayuri,[1] Todd W. Geders,[2] Janet L. Smith,[2] and Richard J. Kuhn[1]*

Markey Center for Structural Biology and Department of Biological Sciences, Purdue University, West Lafayette, Indiana 47907,[1] *and Life Sciences Institute and Department of Biological Chemistry, University of Michigan, Ann Arbor, Michigan 48109*[2]

Received 1 February 2008/Accepted 7 May 2008

The plus-strand RNA genome of Sindbis virus (SINV) encodes four nonstructural proteins (nsP1 to nsP4) that are involved in the replication of the viral RNA. The ~800-amino-acid nsP2 consists of an N-terminal domain with nucleoside triphosphatase and helicase activities and a C-terminal protease domain. Recently, the structure determined for Venezuelan equine encephalitis virus nsP2 indicated the presence of a previously unrecognized methyltransferase (MTase)-like domain within the C-terminal ~200 residues and raised a question about its functional importance. To assess the role of this MTase-like region in viral replication, highly conserved arginine and lysine residues were mutated to alanine. The plaque phenotypes of these mutants ranged from large/wild-type to small plaques with selected mutations demonstrating temperature sensitive lethality. The proteolytic polyprotein processing activity of nsP2 was unaffected in most of the mutants. Some of the temperature-sensitive mutants showed reduction in the minus-strand RNA synthesis, a function that has not yet been ascribed to nsP2. Mutation of SINV residue R615 rendered the virus noncytopathic and incapable of inhibiting the host cell translation but with no effects on the transcriptional inhibition. This property differentiated the mutation at R615 from previously described noncytopathic mutations. These results implicate nsP2 in regulation of minus-strand synthesis and suggest that different regions of the nsP2 MTase-like domain differentially modulate host defense mechanisms, independent of its role as the viral protease.

Sindbis virus (SINV) is the prototype alphavirus of the family *Togaviridae*. Members of this family have a plus-strand RNA genome of about 12 kb in length (68) and include important animal and human pathogens (29, 70, 78). Alphaviruses are transmitted to vertebrate hosts primarily by mosquito vectors. In vertebrate hosts an acute disease, characterized by high-titer viremia, develops and elicits a strong immune response (28). SINV can replicate lytically in most mammalian cell lines while establishing a chronic infection in mosquito cell lines (70).

Upon virus entry, the 11.7-kb SINV genome is translated by the cellular translational machinery into nonstructural proteins nsP1 to nsP4 encoded by the 5′ two-thirds of the genome. These proteins, along with unknown host factors, form the replicase/transcriptase complex responsible for replication of the viral genome and transcription of the viral subgenomic RNA, which is coterminal with the 3′ one-third of the genome and codes for the structural proteins (68, 69). In mammalian cell lines, SINV replication has been shown to lead to development of cytopathic effects (CPE) and cell death by 24 to 48 h postinfection (22). The CPE is a culmination of several physiological and morphological changes caused by the virus infection (34). Using replicons (viral genomes that lack structural proteins), it has been shown that structural proteins are dispensable for both genome replication and for development of CPE (22), thereby implicating the nonstructural proteins in cytopathogenicity.

Each of the nonstructural proteins has a defined role(s) in viral RNA replication. nsP1 is the methyltransferase (MTase) and guanylyltransferase involved in capping the viral RNA (3, 10, 45, 75). nsP1 is also thought to interact with nsP4, contribute to initiation of minus-strand RNA synthesis, and target the replication complex to the plasma membrane (18, 19, 60, 64, 66, 77). Although the precise function of the phosphoprotein nsP3 in viral RNA replication is unknown, the conserved N-terminal region of this protein has been shown to be important in minus-strand RNA and subgenomic RNA synthesis (11, 39, 52, 76). nsP4 is the viral RNA-dependent RNA polymerase and has also been shown to possess terminal adenylyl transferase activity that is involved in adding the poly(A) tail at the 3′ end of the genome (73).

nsp2 is a multifunctional protein (Fig. 1). The N-terminal half functions as the viral RNA helicase (26), RNA-dependent 5′ triphosphatase, and nucleoside triphosphatase (56, 74). The C-terminal region of nsP2 functions as a cysteine protease that sequentially cleaves the nonstructural polyprotein into individual nonstructural proteins (13, 14, 32, 33, 42, 43). Each cleavage gives rise to a polyprotein intermediate with distinct roles in minus- or plus-strand RNA synthesis (40, 41, 65). The first cleavage at the 3/4 junction gives rise to P123 and cleaved nsP4, and this complex functions in minus-strand RNA synthesis.

* Corresponding author. Mailing address: Department of Biological Sciences, 915 W. State St., Lilly Hall of Life Sciences, Purdue University, West Lafayette, IN 47907-1393. Phone: (765) 494-1164. Fax: (765) 496-1189. E-mail: kuhnr@purdue.edu.

† Supplemental material for this article may be found at http://jvi.asm.org/.

▽ Published ahead of print on 21 May 2008.

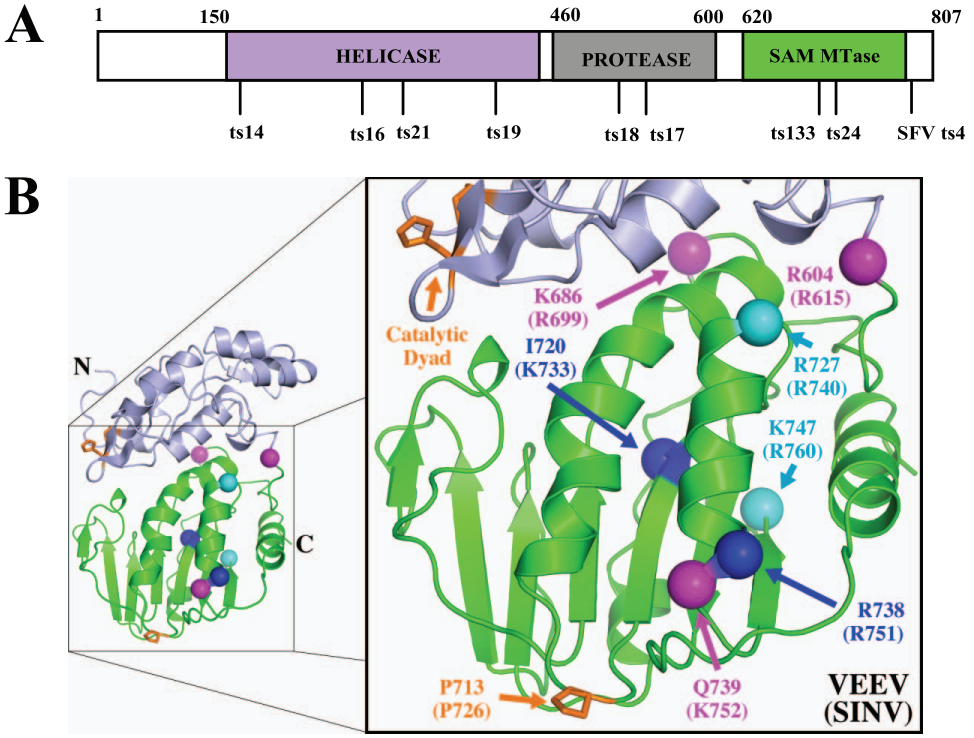

FIG. 1. (A) Schematic for the functional organization of nsP2 in the genus *Alphavirus*. The temperature-sensitive mutations (*ts*) that have been previously mapped to nsP2 helicase, protease, and the MTase-like domain are indicated. Mutations *ts*14, *ts*16, *ts*21, and *ts*19 are located in the helicase domain (62), and mutations *ts*18, *ts*17, *ts*133, and *ts*24 map to the protease domain (30). SFV *ts*4 is another mutation mapped to the extreme C terminus of nsP2 in SFV (71). (B) Location of the SINV nsP2 MTase-like domain residues chosen for mutagenesis on the VEEV nsP2pro structure. The N-terminal protease domain (residues 468 to 603) is shown in gray. The C-terminal MTase-like domain (605 to 787) is depicted in green. The mutated residues are labeled with VEEV numbering and SINV numbering in parentheses. The residues that were mutated in SINV are labeled with the VEEV numbering; e.g., SINV R615 is shown as VEEV R604 (Table 1). The residues are colored based on the plaque phenotype of the corresponding alanine mutants in SINV. Small plaque, blue; medium plaque, cyan. The *ts* lethal mutants are in magenta. The protease catalytic dyad and the residue that corresponds to the previously reported (23) noncytopathic mutation in SINV (SINV P726/VEEV P713), SIN/G, are indicated in orange.

Next, cleavage of the 1/2 junction leads to formation of plus- and minus-strand RNA replicase. Finally, cleavage of the 2/3 site generates a replicase complex solely involved in plus-strand RNA synthesis. A role for host proteins/factors in the switch from early to late stages of replication of the viral RNA has also been suggested (61, 63). Temperature-sensitive mutations mapping to the N-terminal region of nsP2 have been found to affect plus-strand RNA synthesis and are referred to as the conversion-defective mutants (4, 12). Other temperature-sensitive mutations mapping to the C-terminal half of the protein have been found to affect the protease activity, subgenomic RNA synthesis, and shutoff of minus-strand RNA synthesis early in SINV infection (31, 35, 61, 62, 71).

In addition to its established role in viral replication, nsP2 has been implicated as a key player in the downregulation of the host cellular synthetic machinery and in events leading to development of a cytopathic infection by SINV. In particular, the adaptive mutations at residue P726 within the SINV nsP2 protease domain has been common to several studies on persistent infection in SINV and Semliki Forest virus (SFV) (1, 16, 21, 23), although persistently replicating virus or replicons from SINV and SFV had adaptive changes in both the helicase and the protease domains (53). In addition, mutations at residue P726 have been used to show that nsP2 is the viral factor responsible for the host translational and transcriptional inhibition in SINV-infected cells (24, 27).

The crystal structure of the Venezuelan equine encephalitis virus (VEEV) nsP2 C-terminal region, nsP2pro (amino acids 468 to 787 in VEEV), revealed the presence of two domains—a cysteine protease domain, which displayed a novel fold, and a MTase-like domain (59). This two-domain region corresponds to amino acids 472 to 801 in SINV nsP2 (see Fig. S1 in the supplemental material). A substrate binding cleft is proposed to exist between the domains near the catalytic dyad of Cys477 and His546 (C481 and H558 in SINV nsP2). The MTase-like domain has an overall significant tertiary structure similarity to *S*-adenosyl L-methionine-dependent MTase structures (e.g., *Escherichia coli* FtsJ and dengue virus NS5). However, there was no significant similarity in the residues that correspond to the *S*-adenosyl L-methionine binding site between nsP2pro and FtsJ MTase, and structural alignment around the binding site was also poor. Both FtsJ and NS5 are 2′-*O*-MTases, and NS5 is involved in the addition of a type 1 cap to the viral RNA (8, 17). The existence of a resident type 0 capping activity in nsP1 makes the presence of an additional type 1 MTase-like domain seem redundant. Additionally, it has been suggested that the nsP2 MTase-like domain is not a functional MTase (61) and may provide a structural base or

scaffold for interactions with other nonstructural proteins or even RNA at one or more stages of viral RNA replication (59, 61).

Although several mutations in the protease and the MTase-like domain have been characterized for multiple defects in the virus life cycle, the possibility of a distinct and independent role for this unexpected MTase-like domain has not been explored. The present study examines the functional significance of the nsP2 C-terminal MTase-like domain for SINV. Considering the multifunctionality of the protein, mutations in the MTase-like domain were investigated for effects on both viral RNA replication and virus-mediated host modulation. The VEEV nsP2pro structure was used as a reference for interpretation of the observed phenotypes with respect to the predicted residue location on the protein. The mutants displayed a spectrum of phenotypes and were significantly affected in virus viability. The phenotypes of mutants that affected viral RNA replication were clearly distinguished from those that affected virus-mediated host inhibition. The phenotypic characteristics of these MTase-like domain mutants show that residues from different regions of nsP2 are involved in early stages of viral RNA replication, particularly minus-strand RNA synthesis. One of the SINV residues, R615, contributed to efficient plus-strand RNA replication, and its mutation led to specific defects in inhibition of host translation, while minus-strand RNA synthesis, protease activity of nsP2, and inhibition of cellular transcription were not severely affected. These results highlight the multiple roles for the nsP2 MTase-like domain in regulation of replication and differential control of virus-host interactions.

MATERIALS AND METHODS

Cell culture and virus stocks. BHK-21 clone 15 cells (BHK-15) and Vero cells obtained from the ATCC were maintained in minimal essential medium (MEM) (Life Technologies) containing 10% fetal bovine serum (FBS). Cells were grown at 37°C in the presence of 5% CO_2. *Aedes albopictus* mosquito cells, C6/36, obtained from ATCC were maintained in MEM supplemented with 10% FBS and 2 mM L-glutamine at 30°C in the presence of 5% CO_2. Virus stocks were obtained by plaque purification and propagated in BHK cells for higher titers at 37°C for 24 h or at 30°C for 48 h for the temperature-sensitive mutants. For plaque assays, 10-fold serial dilutions of culture supernatant were made in phosphate-buffered saline (PBS) containing 1% FBS. Cells at a density of 80 to 90% were inoculated with the serial dilutions. After infection at 37°C for 1 h, monolayers were overlaid with MEM containing 5% FBS and 1% agarose. The infected cells were incubated at 30°C for 48 h or at 37°C for 24 h, and plaques were visualized by staining with neutral red at a final concentration of 4% in PBS.

Plasmids and cloning procedures. The nsP2 mutations were generated in pToto64, a full-length infectious cDNA clone of SINV that has been previously described (49), using standard overlap PCR mutagenesis procedures.

RNA transcription and transfection. RNA transcripts of SINV were generated by in vitro transcription using SP6 RNA polymerase (Amersham Biosciences) from DNA templates linearized by digestion with SacI restriction enzyme in the presence of the $m^7G(5')ppp(5')G$ cap analog (NEB). This RNA was used for transfection into BHK-15 cells using DEAE-dextran (at 0.2 mg/ml; Sigma-Aldrich) as described previously (38). The transfected cells were assayed for the presence of infectious virus using a standard plaque assay. Viable mutants were plaque purified to generate viral stocks. For electroporation of RNA into BHK-15 cells, subconfluent monolayers of cells grown in T-75 culture flasks ($\sim 1.5 \times 10^7$ cells) were harvested by the addition of trypsin and washed twice with PBS before final resuspension in 400 μl of PBS. The resulting cells were combined with the in vitro transcribed RNA, placed in a 2-mm gap cuvette (Bio-Rad), and electroporated (two pulses at settings of 1.5 kV, 25 μF, and 200 W) using a GenePulser II apparatus (Bio-Rad). Following a 5-min recovery at room temperature, cells were resuspended in MEM supplemented with 10% FBS and dispensed.

Analysis of nsP2 proteolytic processing. In vitro translation and processing analysis was carried out using the SP6 TNT coupled transcription and translation rabbit reticulocyte lysate system (Promega) according to the manufacturer's instructions. The reactions mixtures were supplemented with 10 μCi of [^{35}S]methionine (>1,000 Ci/mmol; GE Healthcare) and 1 μg of plasmid DNA per 25 μl of reaction mixture, and they were incubated for 90 min at 30°C. The reaction products were separated by sodium dodecyl sulfate–10% polyacrylamide gel electrophoresis (SDS-PAGE) and visualized by autoradiography using a phosphorimager (Molecular Imager FX; Bio-Rad). Expression and processing of nonstructural proteins in vivo was analyzed by performing Western immunoblot analysis on lysates of BHK-15 cells infected with wild-type or mutant virus at a multiplicity of infection (MOI) of 5 or electroporated with Toto64 RNA. At 12 h after infection or electroporation, cells were washed with PBS and harvested. Samples were separated under denaturing conditions by SDS-PAGE. The gel was electroblotted onto a nitrocellulose membrane and probed with polyclonal rabbit anti-nsP2 antibody (a generous gift from James Strauss, Caltech) and with an Alexa-Fluor 680-conjugated goat anti-rabbit secondary antibody (Molecular Probes). Bands corresponding to nonstructural proteins were visualized using an Odyssey scanner (LI-COR, Lincoln, NE). Protein (nsP2) levels in the corresponding bands were quantified using Odyssey version 1.1 software.

Analysis of viral RNA replication. Relative levels of plus-strand RNA in infected cells were analyzed as described previously (36). Briefly, two sets of BHK-15 cells were infected with wild-type or mutant virus at an MOI of 10. After infection at 37°C for 1 h, the inoculum was removed, and MEM prewarmed to 30°C and containing 5% FBS and 2.5 μg/ml of actinomycin D was added. The infected cells were either maintained at 30°C throughout the time, or one set was shifted to 37°C after 2 h. Infected cells were then labeled with inorganic ^{32}P (100 μCi/ml) in the presence of actinomycin D (1 μg/ml). Cytoplasmic RNA was extracted at 10 h postinfection. About 2 μg of total RNA was denatured in the presence of formamide-formaldehyde and analyzed by electrophoresis in 1× morpholinepropanesulfonic acid (MOPS) electrophoresis buffer (20 mM MOPS, pH 7.0, 2 mM sodium acetate, 1 mM EDTA, pH 8.0) on a 1% agarose gel containing 2.2 M formaldehyde. Gels were dried and visualized by autoradiography using a phosphorimager (Molecular Imager FX; Bio-Rad). The radioactivity counts in the genomic and subgenomic RNA bands were quantitated using Quantity One software (Bio-Rad).

Analysis of minus-strand RNA synthesis. To detect the levels of minus-strand RNA in infected cells, a minus-strand-specific reverse transcriptase PCR (RT-PCR) assay was used. BHK cells were infected with wild-type or mutant viruses at an MOI of 10. The infected cells were incubated at 37°C, and at specific intervals postinfection (indicated in the figure legends) cytoplasmic RNA was extracted from the infected cells using an RNeasy mini kit (Qiagen) according to the manufacturer's instructions and treated with RQ1 RNase-free DNase I (Promega) at 37°C for 60 min at 40 U/ml of reaction volume. The RNA samples were purified using the manufacturer's protocols (Qiagen) and were used in a two-step minus-strand-specific RT-PCR. RNA (~100 ng) was denatured at 98°C for 2 min, chilled on ice, and allowed to anneal with the plus-sense primer annealing to nucleotides 1 to 42 of the SINV genome (5′-ATTGACGGCGTA GTACACACTATTGAATCAAACAGCCGACCA-3′) at 65°C for 5 min. Con-

TABLE 1. Plaque phenotypes at permissive and nonpermissive temperatures of growth

VEEV nsP2 residue	SINV nsP2 mutation[a]	Plaque phenotype[b]	
		30°C	37°C
R604	R615A	Medium	NP
K646	K658A	Large	Large
M647	R659A	Large	Large
K673	R686A	Large	Large
K686	R699A	Medium	NP
I720	K733A	Medium	Small
R727	R740A	Large	Medium
R738	R751A	Small	Small
Q739	K752A	NP	NP
K747	R760A	Large	Medium
K767?	R781A	Large	Large
R769	R783A	Large	Large
	SINV (wild-type)	Large	Large

[a] The SINV residue analogous to the respective VEEV residue is given in each case.

[b] Plaque sizes are defined as follows: large, 2.0 to 2.5 mm; medium, 1.0 to 2.0 mm; small, ≤0.5 mm. NP, no plaques after 24 h at 37°C or 48 h at 30°C.

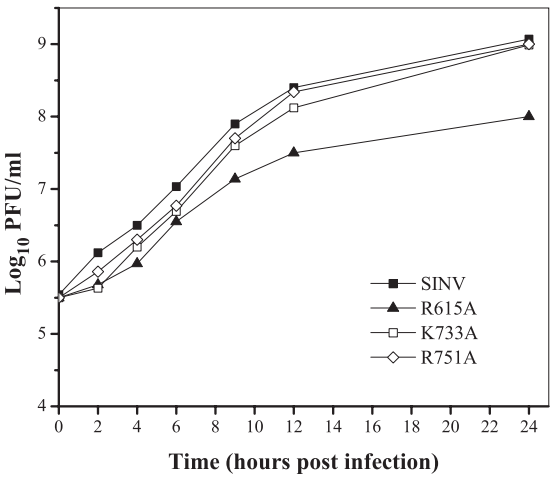

FIG. 2. Analysis of growth and viability for nsP2 MTase-like domain mutants. BHK-15 cells were infected with wild-type (SINV) or mutant virus at the same MOIs. The lethal mutants R615A and R699A, as well as the small-plaque mutants K733A and R751A, were compared with wild-type virus for relative growth rates. At the indicated times, medium was replaced, virus titers were determined by a standard plaque assay, and incubation was carried out at 30°C for 48 h. R699A did not show any detectable virus release.

tents of this tube were mixed on ice with 25 U of avian myeloblastosis virus RT (Promega) and 3 U of RNaseout (Invitrogen) and incubated at 42°C for 30 min, followed by inactivation of RT at 90°C for 5 min. One-tenth of the resulting cDNA product was then used in a PCR with the minus-sense primer that anneals to nucleotides 1617 to 1635 of the SINV genome (5′-CCCCTCCACTTCGCA GACAACTTCTGCGGCTGCCTCGATGCC-3′), with a 30-cycle amplification (unless indicated otherwise). The products were electrophoresed on a 1.2% Tris-borate-EDTA agarose gel, stained using ethidium bromide, and visualized on a Kodak image station 2000R using Molecular Imaging Software, version 4.0. Lambda phage DNA digested with HindIII was used for size quantitation standards.

A dsRNA control for minus-strand specific RT-PCR. Double-stranded RNA (dsRNA) corresponding to the 5′-terminal ~3.0 kb of SINV genomic RNA was prepared in vitro as described previously (65). Briefly, the 5′ terminal 3,051-nucleotide region of SINV was cloned between the SalI and SacI restriction sites on pGEM4Z (Promega). The cloned DNA was linearized with AclI, and plus- and minus-sense RNA were transcribed using SP6 and T7 RNA polymerases (Ambion) in the same reaction at 37°C for 120 min. Template DNA was removed by DNase I treatment at 37°C for 60 min. After DNase treatment, the RNA sample was heated at 70°C for 5 min and annealed by gradual cooling to room temperature. The dsRNA was then treated with RNase A (0.02 mg/ml of the reaction volume) at 37°C for 25 min. The dsRNA was serially diluted in water and used in the two-step RT-PCR as described above. Negative controls included a one-step PCR performed without initial denaturation of the dsRNA or performed without a reverse transcription step.

Analysis of cellular translation. Cellular translation in infected cells was analyzed as described previously (27). Briefly, BHK cells were infected with wild-type or mutant viruses at an MOI of 10 in PBS supplemented with 1% FBS for 1 h. Infected cells were maintained at 37°C in MEM with 5% FBS. At 6 h and 12 h postinfection, the cells were washed with PBS and then incubated for 30 min at 37°C in 0.8 ml of Dulbecco's modified Eagle's medium lacking methionine but supplemented with 0.1% FBS and 20 μCi of [^{35}S]methionine/ml. Then, cells were scraped from the dish into the incubation medium, pelleted by centrifugation, and dissolved in Laemmli (reducing) loading buffer for protein electrophoresis. Samples were electrophoresed on SDS–10% polyacrylamide gels. After electrophoresis, gels were dried, autoradiographed, and analyzed on a phosphorimager (Molecular Imager FX; Bio-Rad). The radioactivity counts in the actin and capsid bands were quantitated using Quantity One software (Bio-Rad) and used to evaluate the host cellular protein synthesis and viral structural protein synthesis, respectively.

Analysis of cellular transcription. BHK-15 cells were infected with viruses at an MOI of 10. At 8 h postinfection, the medium was replaced with MEM containing 5% FBS and inorganic ^{32}P (100 μCi/ml). After 3 h of incubation at 37°C, total RNA was isolated using an RNeasy mini kit (Qiagen) according to the manufacturer's instructions, denatured in the presence of formamide-formaldehyde, and analyzed by electrophoresis in 1× MOPS electrophoresis buffer on a 1% agarose gel containing 2.2 M formaldehyde. Following electrophoresis, gels were dried and visualized by autoradiography using a phosphorimager (Molecular Imager FX; Bio-Rad). The radioactivity counts in the 18S rRNA band were quantitated using Quantity One software (Bio-Rad) and compared with those obtained from uninfected cells.

RESULTS

Mutations in the nsP2 MTase-like domain affect virus viability. The functional role of the nsP2 MTase-like domain of SINV nsP2 was investigated by individual substitutions of alanine for highly conserved lysine and arginine residues in the domain (residues 615 to 807 of SINV nsP2) and characterization of each mutation for its effect on plaque phenotype. The pToto64 cDNA carrying the mutations was transcribed in vitro, and BHK cells were transfected with the in vitro transcribed RNA to determine the effect on virus viability in terms of plaque phenotype. The plaque phenotypes observed at the

TABLE 2. Phenotypic characteristics of MTase-like domain mutants

Virus	Virus titer (PFU/ml) at 37°C[a]	Proteolytic processing (in vitro)[c]	nsp2 synthesis in vivo (37°C)	Percentage of RNA synthesis[e]		Minus-strand synthesis at 6 h[f]
				G	Sg	
SINV	1.2×10^9	+	+	100	100	+++
R615A	4.0×10^{8}[b]	+	+	5	4.1	++
R699A	−	+	−	4.2	4.9	+
K733A	0.8×10^9	I	I	36.8	24	++
R751A	1.0×10^9	+	+	33.5	71	++
R740A	1.2×10^9	+	+	~98	~94	ND
R760A	1.1×10^9	+	+	~98	~90	ND
SIN/G	0.94×10^9	ND[d]	+	ND	ND	ND
SIN/2V	0.82×10^9	ND	I	ND	ND	ND

[a] Virus titers were determined by maintaining infected BHK cells under liquid medium at 37°C for 24 h, harvesting the medium, and assaying the production of progeny viruses by standard plaque assay.
[b] For R615A and R699A plaque analysis was performed at 30°C for 48 h. −, no detectable infectious virus released or no detectable protein synthesis.
[c] I, polyprotein intermediates observed in addition to full length nsP2.
[d] ND, not determined.
[e] Percent incorporation of inorganic [32]P into the genomic (G) and subgenomic (Sg) RNA at 10 h p.i. at 37°C.
[f] Minus-strand synthesis levels: +++, 100%; ++, ~50–100%; +, ~1–10%.

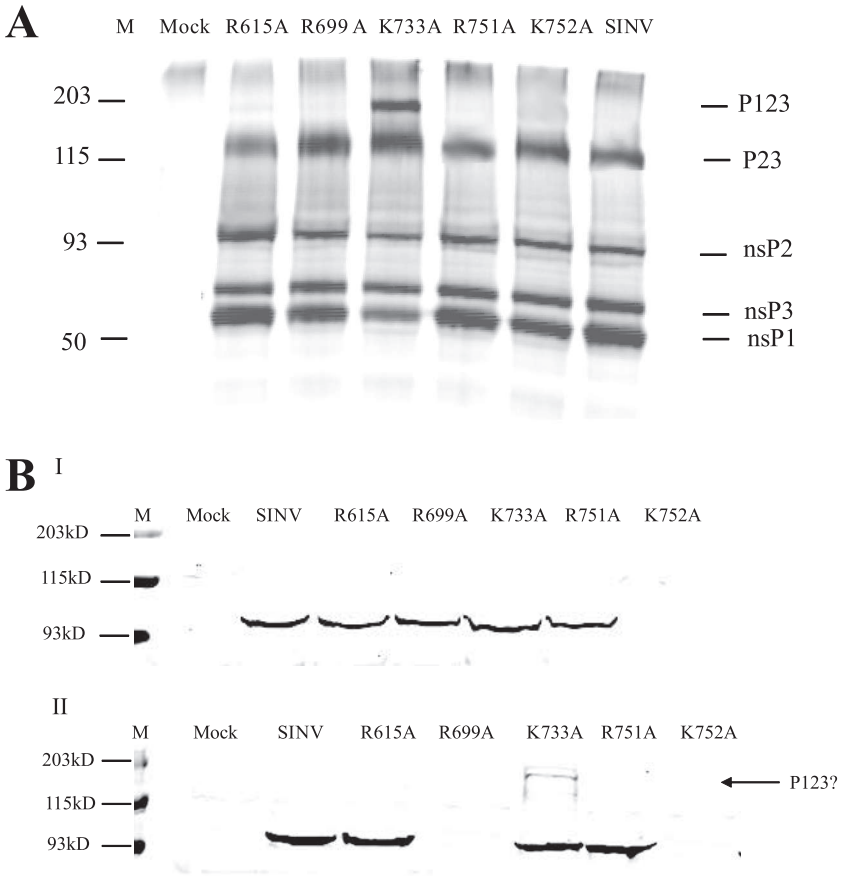

FIG. 3. Analysis of protein synthesis and processing. (A) In vitro transcription and translation of nsP2 lethal (R615A, R699A, and K752A) and small-plaque mutants (K733A and R751A) using the rabbit reticulocyte lysate. Translation products were separated by SDS-PAGE and visualized by autoradiography. Locations of the proteins are indicated on the right. M indicates molecular mass (kDa). (B) Synthesis and processing of nsP2 in virus-infected cells. BHK cells in six-well plates were infected with wild-type (SINV) or mutant virus at an MOI of 5 and incubated at 30°C (I) or 37°C (II). At 12 h postinfection, cells were harvested and equal amounts of proteins were separated by SDS-10% PAGE. After transfer, the nitrocellulose membranes were processed by rabbit anti-nsP2 antibodies and an Alexa-Fluor 680-conjugated goat anti-rabbit secondary antibody (Molecular Probes). The K752A lane represents extracts obtained 12 h postelectroporation with Toto64 RNA carrying the mutation, which was tested previously along with mock and wild-type controls in a separate experiment.

permissive (30°C) and the nonpermissive (37°C) temperatures are summarized in Table 1. Wild-type virus produced large plaques, and 5 of the 12 mutated residues displayed noticeable plaque phenotypic defects. Mutation of residues R615 and R699 yielded no plaques at the nonpermissive temperature, and medium-sized plaques were obtained at the permissive temperature, indicating that these may be temperature-sensitive lethal mutants. Small plaques were obtained for K733A and R751A while medium plaques were seen for the R740A and R760A mutations at the nonpermissive temperature. No plaques were observed at either temperature upon mutation of residue K752. The lethal and small-plaque phenotype for K752A and R751A, respectively, were temperature independent.

The relative replication rates of the mutant viruses in BHK cells were examined in a growth curve analysis (Fig. 2). This experiment included all the mutants that showed a defective plaque phenotype and for which virus could be propagated to high titers at either 30°C or 37°C. SINV wild type produced about 1.2×10^9 PFU/ml after 24 h at 37°C. For the mutants R615A and R699A that had yielded no plaques at the nonpermissive temperature, virus release at 37°C was determined in plaque assays at 30°C. As evident from the growth curve, although R615A was incapable of forming plaques at the nonpermissive temperature, the virus released was infectious, and the titer was reduced by only about 1 log PFU/ml compared to the growth curve for the wild-type virus. However, R699A showed no detectable virus release at 37°C. The small-plaque mutants K733A and R751A showed slightly reduced growth rates at the earlier time points, and the plaques were always reduced in size. Mutants R740A and R760A displayed growth rates and virus titers indistinguishable from the wild type (Table 2). All the mutants were also tested for viability on Vero cells (African green monkey kidney cells) and C6/36 mosquito cells. The plaque phenotypes for the mutants in Vero cells were identical to those observed in BHK cells. The culture supernatant from infected C6/36 mosquito cells maintained at 30°C was used in plaque assays on C6/36 cells at 30°C and on BHK cells at 30°C and 37°C. Despite use of the arthropod host cell line for virus propagation, the mutants displayed temperature sensitivity and altered growth characteristics and retained the respective plaque phenotype that was observed in

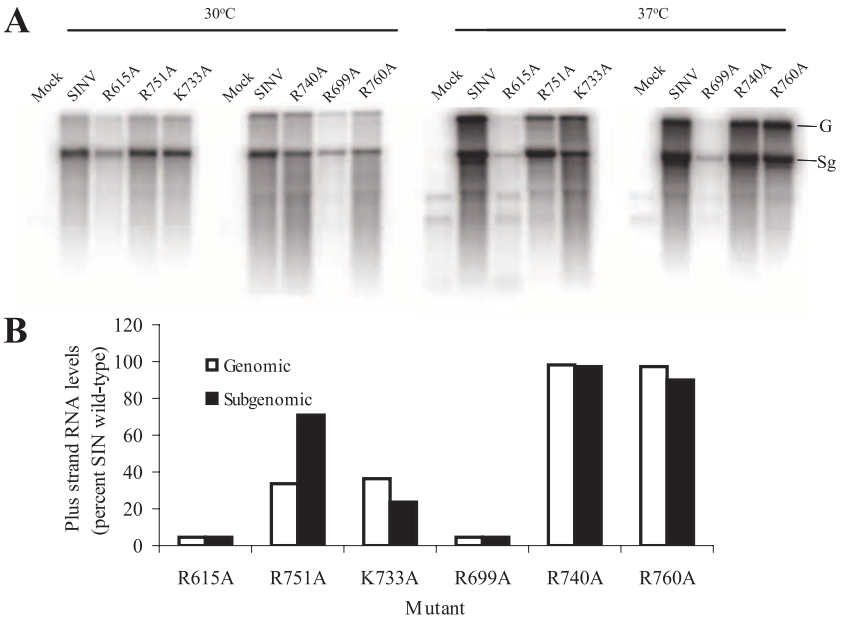

FIG. 4. Analysis of plus-strand RNA synthesis in BHK cells infected with wild-type (SINV) or mutant viruses. (A) The infected cells were maintained at the permissive (30°C) or nonpermissive temperature (37°C) and radiolabeled with inorganic ^{32}P in medium containing actinomycin D. At 10 h postinfection, cytoplasmic RNA was extracted. Approximately 2 μg of total RNA was subjected to denaturing gel electrophoresis on a formaldehyde-agarose gel, and the gel was dried and autoradiographed on a Molecular Imager FX Phosphorimager. (B) The radioactivity counts in bands corresponding to the genomic and subgenomic RNA were quantitated using Quantity One software (Bio-Rad) and used to evaluate the percent RNA levels for the mutants with respect to wild-type virus at 37°C.

BHK cells. This result indicated that the effect of the mutations on the viability of the virus was not cell type specific. These mutants were then examined for possible effects on the efficiency of proteolytic processing of the nonstructural polyprotein and viral RNA replication.

Proteolytic processing of the nonstructural polyprotein. The MTase-like domain mutants were screened for replication-independent defects in protein synthesis and nsP2-mediated processing of the nonstructural polyprotein in vitro using the TNT coupled transcription and translation rabbit reticulocyte system (Promega). A representative gel of the processing activity of the mutants at 30°C following a 90-min reaction is shown in Fig. 3A. Only K733A showed the presence of precursor nonstructural proteins in addition to the fully processed nsP1, nsP2, and nsP3, indicating delayed or reduced processing abilities. All the other mutants with defective plaque phenotypes showed processing results that were indistinguishable from the wild-type (SINV).

To assess the synthesis and processing of nonstructural polyproteins in vivo during the course of the virus infection, BHK cells were infected with the mutant or the wild-type virus at the same MOI at 30°C or 37°C for 12 h. In vitro transcribed RNA (wild type or carrying the mutation) was electroporated into BHK cells to analyze the K752A mutation since virus stocks could not be generated for this mutant. The synthesis and processing of viral nonstructural proteins was analyzed by immunoblotting with polyclonal anti-SINV nsP2 antibodies. The immunoblot analysis (Fig. 2B) showed that both the lethal mutant K752A and the temperature-sensitive lethal mutant R699A displayed negligible levels of nsP2 protein at 37°C compared to nsP2 synthesis in wild-type-infected or -transfected cells. However, nearly wild-type protein levels were detected at both 30°C and 37°C for R615A, R751A (small plaque), R740A, and R760A (both medium-large plaques). Only K733A showed reduction in the efficiency of proteolytic processing, as seen by the presence of a polyprotein precursor in addition to fully processed nsP2. Absence of a predominant polyprotein intermediate suggested that none of the mutations altered the cleavage efficiency at a specific (nsP3/4, nsP1/2 or nsP2/3) cleavage site on the nonstructural polyprotein. The mutation G806V (referred to as SIN/2V) in nsP2, which blocks cleavage at the 2/3 site (27) was used as a control for specific cleavage defects (Table 2 and data not shown).

The lethal mutants (R699A and K752A) did not display altered processing in vitro but showed negligible protein synthesis during the course of virus infection. The mutant R615A displayed almost wild-type levels of polyprotein synthesis and its processing under replication-independent in vitro conditions as well as during virus replication at the nonpermissive temperature. Translation of the incoming RNA in a viral infection and replication of the viral RNA by the translated nonstructural proteins are interdependent events during the early stages of infection. These mutants were differentially characterized for possible defects in plus- and minus-strand RNA replication.

Analysis of plus-strand RNA replication. The relative levels of radiolabeled genomic and subgenomic RNA in cells infected with the mutants were used as an indication of the plus-strand RNA synthesis. The mutants once again displayed a range of phenotypes (Fig. 4). The medium-plaque mutants, R740A and R760A, displayed almost wild-type levels for both genomic and subgenomic RNA (>90% of wild-type virus). Among the small-plaque mutants, K733A had reduced genomic and

subgenomic RNA (~37% and 24%, respectively). R751A showed appreciable levels of subgenomic RNA synthesis (71% of wild type), but genomic RNA was almost as low as K733A (34%), which indicated a specific role for the residue R751 in genomic RNA synthesis. The temperature-sensitive lethal mutant R699A displayed noticeably reduced levels for both genomic and subgenomic RNA at the nonpermissive temperature (4 to 5% of wild-type replication levels), while at the permissive temperatures of growth, the RNA levels were not as severely reduced. The plus-stand RNA synthesis for R615A was also noticeably reduced at the nonpermissive temperature and was, in fact, comparable to the levels observed for the temperature-sensitive lethal mutant R699A. In this context the mutants from this study differed substantially from the previously characterized temperature-sensitive mutants in the nsP2 proteases and MTase-like domains of SINV and SFV that have been shown to cause specific defects in subgenomic RNA synthesis with no effects on genomic RNA synthesis (4, 71). The mutants were then compared for the efficiency of minus-strand RNA synthesis to account for the reduced plus-strand RNA levels.

Analysis of minus-strand RNA synthesis. Minus-strand RNA from infected cells was found as a part of dsRNA structures (replicative intermediate or replicative form) when isolated from infected cell lysates that were deproteinized and the RNA was collected by ethanol precipitation (67). To detect the levels of minus-strand RNA in infected cells, a minus-strand-specific RT-PCR assay was used as previously described (65). To determine the detection limit of the RT-PCR assay, dsRNA representing the 5′-terminal 3,051-nucleotide region of SINV was produced in vitro. This in vitro synthesized dsRNA was subjected to a minus-strand RNA-specific RT-PCR designed to amplify a 1,633-bp region. The intensity of the PCR product detected increased with increasing input RNA for up to about 10^6 molecules of dsRNA before becoming saturated, indicating that the assay could be used to detect molecules of minus-strand RNA in the range of about a 100 to 10^6 molecules (Fig. 5A). To detect minus-strand RNA synthesis in vivo, BHK cells were infected with wild-type or lethal/small-plaque mutant viruses at an MOI of 10. The infected cells were incubated at 37°C, and at various times after infection/transfection, cytoplasmic RNA was extracted from the infected cells and used in the minus-strand-specific two-step RT-PCR assay.

The negligible levels of minus-strand RNA for all the time points examined in cells infected with R699A indicated that the mutant protein was incapable of efficient minus-strand synthesis (Fig. 4B). The mutant K752A displayed no detectable minus-strand RNA synthesis up to about 6 h postinfection, but a faint band was observed for minus-strand RNA at 12 h postinfection (Fig. 4C), suggesting slow recovery or reversion. The mutant R615A, however, displayed a less severe defect in minus-strand RNA synthesis than mutants R699A and K752A. The levels for minus-strand RNA-derived PCR product though reduced showed an increase in intensity by 6 h postinfection, in contrast to the other lethal mutants (Fig. 4B). The small-plaque mutants K733A and R751A showed low levels of minus-stand RNA at 1 h and 3 h postinfection (Fig. 4D), reflecting reduced minus-strand RNA synthesis, which is also reflected in the slow growth of these viruses (Fig. 2); but by 6 h the RNA levels had reached saturation, and any possible differences between wild-type and mutant viruses could not be ascertained.

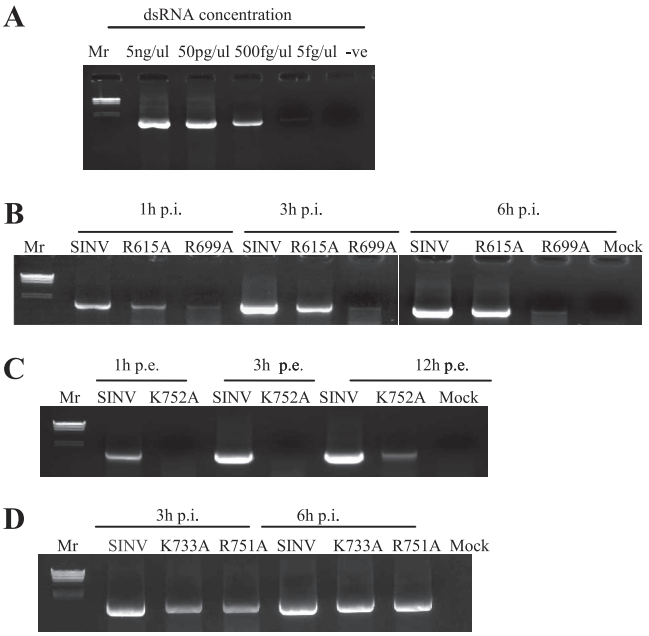

FIG. 5. Detection of minus-strand RNA by RT-PCR. (A) dsRNA was prepared by hybridizing plus-sense and minus-sense in vitro transcripts representing the 5′ terminal 3.0-kb region of the SINV genome. The dsRNA was serially diluted in water (the concentration of RNA is shown at the top) and used in a minus-strand-specific RT-PCR assay to amplify a 1.6-kb fragment; -ve, one-step RT-PCR negative control. (B, C, and D) Minus-strand-specific RT-PCR for cytoplasmic RNA derived from cells infected with wild-type (SINV) or mutant virus at an MOI of 10 (B and C) or transfected with 10 μg of RNA carrying the mutation (D). The PCR amplification was for 30 cycles except in the case of K733A and R751A (C), where the amplification was 15 cycles long for the 6-h time point. Lambda phage DNA digested with HindIII was used for size standards (M_r). Cytoplasmic RNA from uninfected cells was used as a control (Mock). p.i. postinfection; p.e., postelectroporation.

The characterization of all the mutants for their ability to synthesize minus-strand RNA indicated that most of the residues examined were critical for efficient minus-strand and therefore plus-strand RNA synthesis. The possible role of these residues in nsP2-mediated downregulation of host cellular translation and transcription was then investigated.

Cytopathogenicity and modulation of host macromolecular synthesis. nsP2 has been associated with virus cytopathogenicity by means of adaptive mutations that have been mapped to both the N-terminal and the C-terminal regions of the protein in noncytopathic variants of SINV and SFV (16, 21, 53). The protein has also been suggested to play a role in host translational and transcriptional shutoff (27). Mutants from this study were analyzed for their ability to induce CPE and inhibit cellular translation and transcription.

BHK cells infected with wild-type or mutant viruses were observed for CPE at 37°C at different times postinfection. While SINV showed complete CPE by 24 h, small-plaque mutants K733A and R751A showed complete CPE by 36 h. R615A showed no detectable CPE at 24 h and only partial CPE at 48 h. Lethal mutant R699A showed no CPE at 37°C.

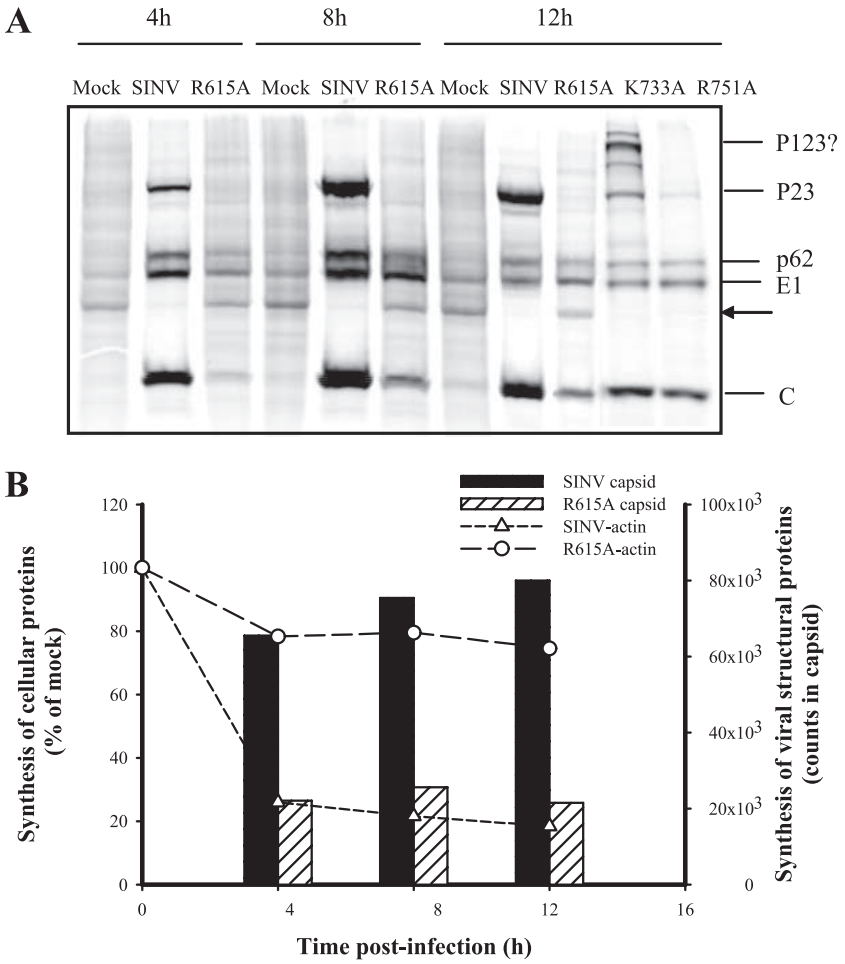

FIG. 6. Virus protein synthesis and inhibition of host cellular translation in cells infected with SINV wild-type or mutant virus. BHK-15 cells were infected at an MOI of 10. (A) At the indicated times, proteins were pulse labeled with [^{35}S]methionine and analyzed on an SDS-10% polyacrylamide gel. Gels were dried and autoradiographed. The positions of SINV structural proteins and uncleaved P23 are indicated. The position of the actin band is indicated by an arrow. (B) Synthesis of cellular proteins in infected cells was analyzed by measuring the radioactivity counts in the actin band (SINV-actin or R615A-actin), and the results were normalized with the radioactivity detected in uninfected cells. Viral protein synthesis in infected cells was evaluated by measuring the radioactivity counts in the band of the capsid protein (SINV-capsid or R615A-capsid).

These results were consistent with previous reports suggesting a direct correlation between the levels of viral replication and the development of CPE (21).

In addition to the development of CPE, another major change accompanying infection of vertebrate cells with SINV is downregulation of transcription and translation of cellular mRNAs, which contributes to suppression of the host antiviral response. The mutants in this study that showed appreciable nsP2 synthesis, reduced replication, and delayed or negligible CPE (R615A, K733A, and R751A) were then tested for inhibition of host translation and transcription.

BHK cells were infected with wild-type (SINV) or mutant viruses at an MOI of 10. The infected cells were incubated at 37°C. At various times postinfection, the infected cells were radiolabeled with [^{35}S]methionine. The radioactive counts from the band for β-actin were used for quantitation of cellular protein synthesis, and the capsid band was used as an indicator of synthesis of viral structural proteins.

Wild-type SINV and small-plaque mutants K733A (polyprotein processing defects) and R751A (reduced RNA replication) displayed comparable and efficient inhibition of cellular translation (Fig. 6). This once again demonstrated that defects in polyprotein processing and RNA replication do not a priori prevent inhibition of cellular translation, as reported previously (23, 27). On the other hand, the mutant R615A displayed reduced efficiency at inhibiting host cellular translation. The cellular protein (actin) synthesis in cells infected with SINV was only about 20% of that from mock-infected cells, but cells infected with R615A had about 80% as much actin synthesis as in mock-infected cells (Fig. 6B). The synthesis of virus structural proteins (capsid protein) in R615A-infected cells was reduced about 3- to 3.5-fold relative to wild-type SINV, which was also seen as a moderate reduction in the release of infectious virus for this mutant at the nonpermissive temperature (Fig. 5). This indicated that the reduced ability of R615A to downregulate the cellular machinery and cause CPE could not be attributed to lack of assembly and release of infectious virus.

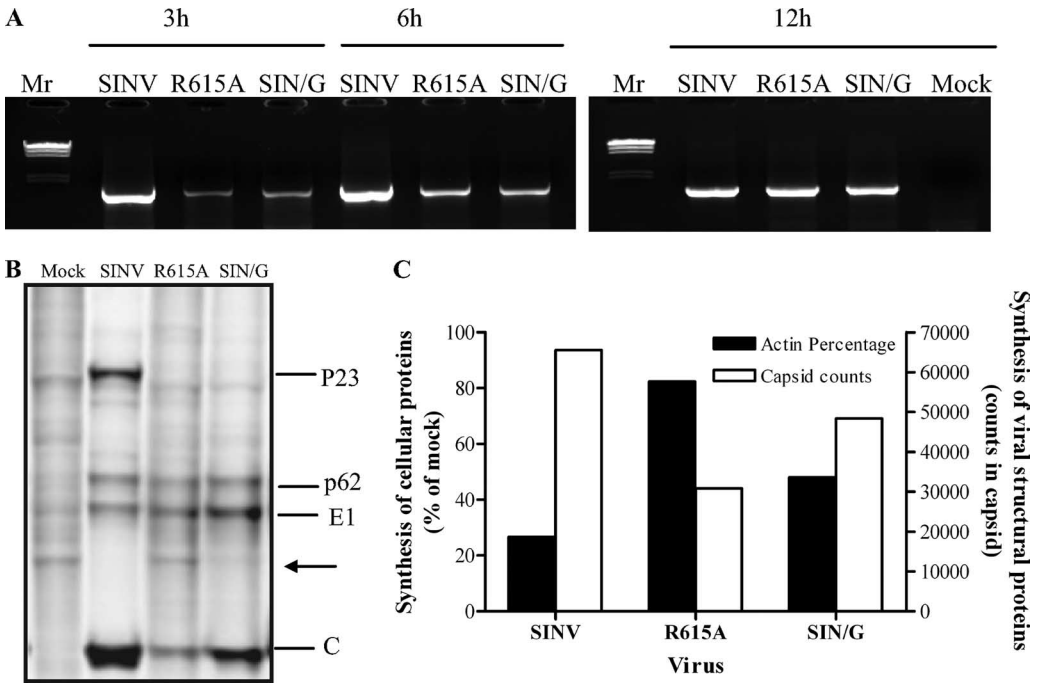

FIG. 7. Comparison of phenotypic characteristics for R615A and SIN/G. (A) Minus-strand RNA synthesis. BHK cells were infected with wild-type virus (SINV), R615A, or the SIN/G mutant at an MOI of 10. At different times postinfection cytoplasmic RNA was extracted and used in a minus-strand-specific two-step RT-PCR as described in Materials and Methods. (B) Comparison of virus and cellular protein synthesis in cells infected with R615A, SIN/G, or wild-type (SINV) virus. BHK-15 cells were infected at an MOI of 10 and maintained at 37°C. At 8 h postinfection proteins were pulse labeled with [^{35}S]methionine at the indicated times and analyzed on an SDS-10% polyacrylamide gel. Gels were dried and autoradiographed. The positions of SINV structural proteins and uncleaved P23 are indicated. The position of the actin band is indicated by an arrow. (C) The synthesis of cellular proteins in infected cells was analyzed by measuring the radioactivity counts in the actin band, and the results were normalized on the amount of radioactivity detected in uninfected cells. Viral protein synthesis in infected cells was evaluated by measuring the radioactivity counts in the band of the capsid protein.

The inability of R615A to shut off host translation as efficiently as wild-type SINV and the lack of CPE in R615A-infected cells were similar to a previously reported adaptive change at position P726 of nsP2 in persistent infections of both SINV and SFV virus and replicons (1, 21, 23). In order to perform a comparative analysis for R615A, the adaptive mutation P726G, referred to as SIN/G (23), was engineered into the SINV infectious cDNA clone. In vitro transcribed RNA was used for transfection, and a standard plaque assay was performed. SIN/G was viable, giving rise to medium-sized plaques on BHK-15 cells at 37°C as opposed to the no-plaque phenotype of R615A at 37°C (Table 2). The medium-plaque phenotype for SIN/G was not surprising since the cytopathic defects for SIN/G are known to be cell line dependent (23). Minus-strand RNA synthesis for both mutants displayed a slow but steady increase that approached wild-type levels by 12 h postinfection (Fig. 7A). The levels of host protein synthesis in SIN/G-infected cells was about 40% of that in mock-infected cells, as opposed to ~20% for cells infected with wild-type SINV and about 80% for R615A-infected cells (Fig. 7B and C). Therefore, R615A caused a more severe defect in the ability of nsP2 to downregulate cellular protein synthesis compared to SIN/G. Synthesis of the viral structural proteins (capsid) was higher for SIN/G than that seen for R615A, consistent with medium plaque size for SIN/G at 37°C.

The transcriptional inhibition profiles for R615A and SIN/G were then compared to further differentiate the two mutants. As seen previously (27), the mock-infected cells displayed the presence of large amounts of 28S rRNA, 18S rRNA, and rRNA precursors. The 18S rRNA band was used as a marker for cellular transcription and processing because the rRNA precursors comigrated with the viral genomic RNA, and 28S rRNA comigrated with the subgenomic RNA. The wild-type virus inhibited cellular transcription such that the 18S rRNA level was about 3% of that from mock-infected cells (Fig. 8). Also, mature 18S and 28S rRNA were barely detectable, while both genomic and the subgenomic RNA could be detected. SIN/G displayed moderate defects in transcriptional inhibition, with 18S rRNA at about 39% of the levels detected in mock-infected cells. Surprisingly, R615A displayed no detectable rRNA precursors or mature cleavage products. The levels of genomic and subgenomic RNA were lower in cells infected with R615A than wild-type SINV, as seen previously (Fig. 3). However, the transcriptional inhibition was unimpaired in R615A-infected cells, with 18S rRNA levels of about 3.5% of the mock-infected cells for both wild-type virus and R615A. These results indicate that R615 and P726 have different roles in modulation of the host.

Roles for conserved residues in the interdomain region. VEEV residue R604 (analogous to SINV R615) (Fig. 1B and Table 1; see also Fig. S1 in the supplemental material) is located on a 29-residue loop that links the protease domain (VEEV residues 468 to 581 and SINV 472 to 592) and the MTase-like domain (VEEV residues 610 to 787 and SINV 621

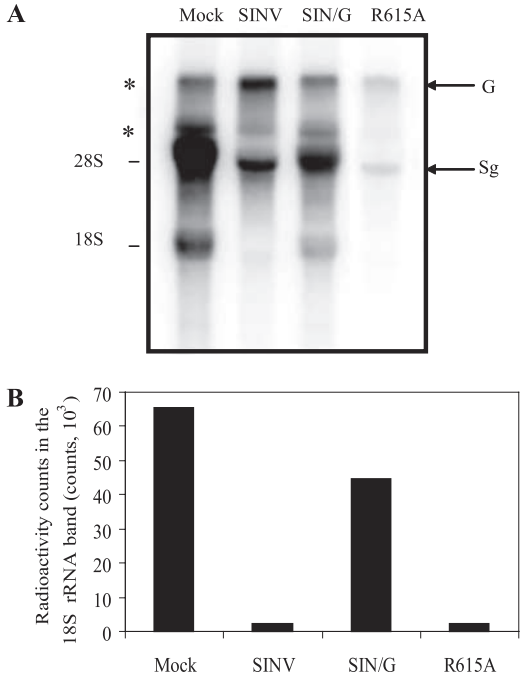

FIG. 8. Inhibition of transcription in cells infected with wild-type or mutant viruses. (A) BHK-15 cells were infected with SINV, R615A, or SIN/G mutants at an MOI of 10 and maintained at 37°C. At 6 h postinfection cellular RNAs were labeled with inorganic ^{32}P for 3 h, and the RNA was extracted and analyzed by gel electrophoresis under the conditions described in Materials and Methods. The positions of 28S and 18S rRNA bands are indicated. G and Sg indicate the viral genomic and subgenomic RNAs, respectively. Asterisks indicate the rRNA precursors. (B) The synthesis of cellular RNA in infected cells was analyzed by measuring the radioactivity counts in the 18S rRNA band.

to 801) (Fig. 1B) (59). The possibility that the phenotypic characteristics of R615A were due to its location in a highly conserved region of this loop (see Fig. S1 in the supplemental material) was examined by mutational analysis. Twelve residues surrounding R615 (SINV 609 to 622) were replaced with alanines, and the effects on virus viability (plaque phenotype at 30°C and 37°C), synthesis of protein, and proteolytic processing were determined. Most of the mutations resulted in large or medium plaques at both temperatures and wild-type levels of nsP2 (Table 3). Three of the mutations led to a no-plaque phenotype at 37°C (N609A, N614A, and L621A), but only the mutant N614A displayed characteristics of a temperature-sensitive plaque phenotype, similar to R615A (Table 3). The no-plaque mutants N609A and L621A displayed no protein (nsP2) synthesis at 37°C; however, N614A had nearly wild-type levels of nonstructural proteins, similar to R615A (Table 3). The mutant L610A displayed a small-plaque phenotype and showed reduced polyprotein proteolytic processing.

Due to the similarities in the phenotypic characteristics of N614A and R615A, the effects of N614A on the inhibition of cellular translation and transcription were determined in parallel with R615A. The two mutations had virtually identical effects. Cells infected with N614A showed 82% of the levels of actin relative to mock-infected cells at 8 h postinfection, similar to 80% in cells infected with the R615A mutation and 20% in SINV wild-type-infected cells, as seen before (Fig. 6). Virus-mediated transcriptional inhibition of the host was once again unaffected in cells infected with either N614A or R615A. These results indicated that invariant residues N614 and R615 have similar roles in virus replication and survival.

DISCUSSION

The nonstructural proteins from several RNA viruses have been found to play multiple roles in virus replication. In addition to being involved in viral RNA genome replication, they act as antagonists of the host response to virus infection. Examples include the NS4B protein in dengue virus (46, 47), the NS5 protein of Japanese encephalitis virus and Langat virus (5, 44), the NS5a protein of hepatitis C virus (reviewed in reference 54), the nonstructural proteins of Rift Valley virus (6), poliovirus proteases 2A and 3C (9, 79), and the influenza virus NS1 protein (15, 72). The mechanism of host inhibition differs significantly among these viruses. The virus may utilize the resident enzymatic activity of a viral protein to downregulate the host response, as in case of the picornavirus proteases (9, 79). Or the host inhibitory function of a viral protein may overlap with a region that is involved in viral RNA replication, like the RNA-dependent RNA polymerase domain of Langat virus (50).

In alphaviruses, two distinct proteins have been found to contribute to virus-mediated host modulation. In the Old World alphaviruses, e.g., SINV and SFV, nsP2 is the protein that is involved in cellular downregulation (16, 21, 23, 27, 53). Recently it was demonstrated that for New World alphaviruses e.g., VEEV and Eastern equine encephalitis virus, virus-mediated host antagonism is a property of the capsid protein (CP) (25), similar to the M (matrix) protein of vesicular stomatitis virus (2, 7). These proteins are involved in different aspects of the virus life cycle, nsP2 in RNA replication and CP in formation of the nucleocapsid core. Both proteins are viral proteases responsible for critical cleavages during the virus infection (70). Unlike picornaviruses, host antagonism in alphaviruses

TABLE 3. Phenotypic characteristics of nsP2 interdomain loop mutants[a]

Mutation	Plaque phenotype	nsP2 synthesis in vivo[b]
SINV	Large	+
N609A	NP	−
L610A	Small	I
V611A	Large	+
P612A	Large	+
V613A	Large	+
N614A*	NP (*ts*)	+
R615A*	NP (*ts*)	+
N616A	Large	+
L617A	Large	+
P618A	Large	+
H619A	Medium	+
A620R	Large	+
L621A	NP	−
V622A	Large	+

[a] Plaque phenotype and nsP2 synthesis represent results obtained at 37°C. Plaque phenotype analysis was also performed at 30°C for all mutants that did not form plaques at 37°C to identify a temperature-sensitive (*ts*) lethal phenotype (*). NP, no plaques.

[b] I, polyprotein intermediates observed in addition to full-length nsP2.

does not depend on viral protease activity (27). Alphavirus nsP2 is a multifunctional protein and also exists in multiple forms. The cytoplasmic form of nsP2 functions in the replicase complex or exists as a soluble factor thought to regulate subgenomic RNA synthesis (71). The nuclear form of the protein is not involved in replication and is important for modulation of the host in the Old World alphaviruses, e.g., SINV and SFV (16, 21, 23, 27, 53).We sought to investigate the functional relevance of the nsP2 MTase-like domain in the diverse roles of nsP2 during viral RNA replication and host cellular shutoff during the viral replicative cycle, with the structure from VEEV nsP2pro as a reference.

Twelve highly conserved lysine and arginine residues in the MTase-like domain of SINV (residues 615 to 807) were mutated to alanines as an initial screen to identify residues important for the virus life cycle. The mutations led to diverse effects on virus viability and replication. The kinetics of virus growth for the small-plaque mutants (K733A and R751A) was only moderately different from the wild-type virus, compared to the more obvious difference in plaque phenotypes (Fig. 2 and Table 2). Differences between plaque phenotypes and growth kinetics have been previously reported for SINV 5′ and 3′ nontranslated region mutants (37, 48) and suggest that subtle changes in growth kinetics have a more significant manifestation on the ability of the virus to form plaques. Most of the residues that affected virus growth in SINV could be mapped to solvent accessible surfaces on the VEEV nsP2pro structure (Table 1 and Fig. 1B). However, not all conserved, surface-exposed, positively charged residues displayed growth defects upon mutagenesis (Table 2). One example was the conserved nuclear localization sequence (657 RKR 659 in SINV nsP2) (51, 57). Single amino acid substitutions of residues K658 or R659 did not lead to altered virus viability, consistent with previous reports (20, 55, 58). Alanine substitutions for SINV nsP2 residues R686, R781, and R783 also had no effect on virus viability (Table 1).

Several previously reported mutations in the protease and MTase-like domain of nsP2 were associated with temperature-sensitive defects in polyprotein processing in both SFV and SINV (62, 71). Recently reported temperature-sensitive mutants in the helicase domain of SFV nsP2 displayed reduced NTPase and processing functions (4). The ability of residues distant from the protease active site to influence the proteolytic processing of the polyprotein made it important to screen the mutants for processing defects. With the exception of K733A, the mutants in this study largely did not seem to alter the nonstructural polyprotein processing activity of nsP2 at the permissive temperature in vitro or at the nonpermissive temperature in infected cells (Fig. 3). The reduced efficiency of proteolysis processing and the decreased levels of subgenomic RNA synthesis seen for the mutant K733A were similar to previously reported nsP2 C-terminal temperature-sensitive mutants (30, 62, 71). The effect of K733A on the protease may arise from disruption of the K733-mediated interactions, which may destabilize the integrity of the MTase-like domain and its contribution to the substrate binding cleft at nonpermissive temperatures. These possibilities could explain the polyprotein intermediates detected for K733A (Fig. 3 and 6A).

While polyprotein precursors arising from defects in processing did not accumulate in cells infected with most of the mutants, the levels of overall nonstructural protein synthesis differed significantly. The reduced protein synthesis for mutants R699A and K752A suggested that these mutations either destabilized nsP2 at nonpermissive temperatures or abrogated a function of nsP2 required during early stages of viral infection. Protein stability defects could be ruled out for K752A since this mutant displayed wild-type levels of protein synthesis at 30°C in vitro (Fig. 3) but not during virus infection in vivo. This indicated that the mutation affected a critical function of nsP2 during replication, which in turn also affected nonstructural protein synthesis. Similarly, R699A showed ~50% recovery of protein synthesis when cells infected with the virus were initially maintained at the permissive temperature for 4 h postinfection, followed by a shift to the nonpermissive temperature (data not shown), suggesting that the temperature sensitivity of this mutant was not because the mutation rendered the protein thermolabile.

Therefore, the mutations R699A and K752A may affect nsP2 functions early in virus replication, resulting in reduced protein synthesis and replication. This early step in viral replication could be minus-strand RNA synthesis. A comparison of plus- and minus-strand RNA synthesis for the mutants revealed that the levels for both genomic and subgenomic RNA were reduced for all the mutants with defects in viability, e.g., R615A, R699A, K733A, and R751A (Fig. 4). The reduction in plus-strand RNA synthesis observed for these mutants could have arisen either from limited availability of minus-strand RNA templates because of an inefficient minus-strand replicase or from defective functioning of plus-strand replicase, similar to the previously characterized nsP2 amino terminal "conversion mutants" (12).

Plus-strand RNA synthesis early in virus replication depends on the ability of a functional minus-strand replicase to utilize the incoming RNA (due to virus infection) as a substrate (63, 65). Mutants with inefficient minus-strand RNA synthesis (defective minus-strand replicase) would adversely affect all downstream events, i.e., plus-strand RNA synthesis and translation of plus-strand RNA into nonstructural polyprotein. In this study, minus-strand replication was downregulated for all mutants that displayed a reduction in the levels of genomic and subgenomic RNA (Fig. 4 and 5). Previously, molecular genetic studies have suggested a role for nsP1 and nsP3 in the synthesis of minus-strand RNA (76, 77). The results from this study indicate that residues in the MTase-like domain may have an important role in the early minus-strand RNA synthesis, either in stabilizing nsP2 interactions in the minus-strand replicase (nsP1, -2, and -3 and nsP4) or even in promoter recognition for minus-strand RNA synthesis. Interaction studies involving all the nonstructural proteins using a combination of biochemical (in vitro) and replication-independent in vivo analysis would help to define precise roles of these residues in early infection.

However, the mutation of SINV residue R615 gave rise to phenotypic characteristics that differed from the other nonviable mutants. The mutant R615A did not give rise to an observable CPE at the nonpermissive temperature but displayed a reduced rate of infectious virus release at this temperature. This mutant did not display remarkable defects in efficiency of nonstructural polyprotein processing compared to wild-type virus (Fig. 3 and 6A). The mutation did, however, affect plus-strand RNA replication. And while the plus-strand RNA levels

for this mutant were comparable to the temperature-sensitive lethal mutant R699A (Fig. 4), the minus-strand RNA levels for R615A did not show the same dramatic reduction as R699A (Fig. 5B). This suggests that residue R615 presumably contributes more significantly to the establishment of a functional replicase complex during plus-strand RNA replication. The synthesis of wild-type levels of nonstructural protein but reduced plus-strand RNA synthesis seen for R615A was similar to the characteristics of SIN/G in NIH 3T3 cells (27).

In addition to its role in viral replication, R615 contributes to virus-host interactions that result in a lytic infection by SINV. The R615A mutant did not affect virus production significantly, indicating that the low levels of replication were enough to produce packaged virus particles that cause a noncytopathic infection (Fig. 2 and 6). Comparison of R615A with the extensively studied persistent infection mutant SIN/G revealed similarities at the level of replication but significant differences in host modulation.

There have been conflicting reports on the levels of minus- and plus-strand RNA synthesis by persistent-infection mutants in SINV and SFV (53, 61). The minus-strand RNA levels were similar for the mutants R615A and SIN/G (Fig. 7A). R615A had a more pronounced effect on the ability of nsP2 to cause host translational shutoff than SIN/G, which showed moderate effects (Fig. 7B and C). On the other hand, while the role of nsP2 in transcriptional inhibition was unaffected for R615A, SIN/G showed less efficient inhibition of cellular transcription (Fig. 8). Previously, nsP2-mediated inhibition of cellular transcription was shown to be affected by the state of nonstructural polyprotein processing and cellular distribution of nsP2 (24, 27). In addition, the inhibition of transcription by nsP2 was suggested to play the more critical role in virus-mediated suppression of the cellular stress response The polyprotein processing (and cellular distribution [data not shown]) by nsP2 in R615A-infected cells had no observable differences from cells infected with wild-type virus (Fig. 3). Therefore, these results implicated the change of the residue R615 in causing defects in translational shutoff with no direct role in nsP2-mediated transcriptional inhibition of the host. This suggests that surface-exposed residues, R615 and P726, in the MTase-like domain have different functions in virus-host interactions. While mutation of P726 leads to an overall reduction in nsP2-mediated interruption of host translation and transcription, the change at residue R615 specifically affects the ability of the virus to inhibit cellular translation.

A careful analysis of the VEEV nsP2pro structure reveals that a 29-residue interdomain linker (SINV 593 to 620 and VEEV 582 to 609) connects the protease and the MTase-like domains (Fig. 1B). This linker region could act as a hinge to allow the two domains to form a functional substrate-binding cleft for the protease. The invariant R615 is surrounded by 12 highly conserved residues (see Fig. S1 in the supplemental material), suggesting that this region may have a common function in virus replication and viability and also raising the possibility that the unique phenotypic characteristics of the mutant R615A (compared to other MTase-like domain mutants) may be attributed to the location of the residue R615 on this loop. Additionally, the surface accessibility of R615 and phenotype for R615A hint at a role for the linker region in mediating virus-host interactions.

Mutational analysis of the 12 residues around R615 revealed that not all of the conserved residues had critical roles in the virus life cycle. However, the phenotypic characteristics for N614A and R615A indicated that these interdomain residues indeed contributed specifically to the protease-independent host translational inhibition by nsP2 and in the cytopathic outcome of SINV infection. Unlike the distribution of function in host antagonism seen for the picornavirus proteases 2A (translational inhibition) and 3C (transcriptional inhibition) (9, 79), the same domain in nsP2 has residues involved in specific aspects of host cellular downregulation. It remains to be determined whether the residues in the nsP2 MTase-like domain control nsP2-mediated transcriptional inhibition in a manner that is independent of the host translational shutoff and the viral protease functions. Comparison of New and Old World alphaviruses reveals that the amino-terminal region of VEEV CP, which is involved in host antagonism, is independent of the protease domain and the major viral RNA-binding domain (25). The VEEV CP amino-terminal region is located between helix I (that contributes to coiled-coil interactions in nucleocapsid core) and the positively charged RNA-binding region. Similarly, we found that in the case of nsP2, residues in the MTase-like domain have specific roles in the virus-mediated host downregulation. This suggests that the virus evolved to mediate interactions with other viral and/or host proteins using structural motifs that do not contribute enzymatically to virus replication (nsP2 MTase-like domain and CP N-terminal region).

In summary, we used point mutations in the SINV nsP2 MTase-like domain to answer questions about its functional significance during viral replication. The phenotypic characteristics of the residues demonstrated the following: (i) that this domain is involved in early stages of viral replication, presumably in the establishment of a stable, functional (minus strand) replicase; (ii) that residues located on the linker between the protease and MTase-like domain have specific roles in host translational inhibition in addition to their roles in viral RNA replication; (iii) that these residues play a critical role in the ability of SINV to give rise to a cytopathic infection, and in contrast to previous reports (27), loss of host translational inhibition may contribute significantly (if not solely) to development of a noncytopathic infection. Mutation of residue SINV R615 gives rise to a virus with all the desired phenotypes of a persistent SINV vector: reduced inhibition of host macromolecular synthesis, reduced vector RNA synthesis, efficient protein synthesis, and efficient packaging into alphavirus particles. Therefore, these results also provide information about residues that can be used for construction of noncytopathic SINV vectors for gene delivery, as well as production of recombinant proteins in cultured cells.

ACKNOWLEDGMENTS

We are grateful to James Strauss for providing anti-SINV nsP2 antibodies. We thank Anita Robinson and Kaice Randall for assistance.

This work was supported by a Public Health Service Program Project Grant (AI55672) from the National Institute of Allergy and Infectious Diseases.

REFERENCES

1. **Agapov, E. V., I. Frolov, B. D. Lindenbach, B. M. Pragai, S. Schlesinger, and C. M. Rice.** 1998. Noncytopathic Sindbis virus RNA vectors for heterologous gene expression. Proc. Natl. Acad. Sci. USA **95:**12989–12994.
2. **Ahmed, M., and D. S. Lyles.** 1998. Effect of vesicular stomatitis virus matrix protein on transcription directed by host RNA polymerases I, II, and III. J. Virol. **72:**8413–8419.
3. **Ahola, T., and L. Kaariainen.** 1995. Reaction in alphavirus mRNA capping: formation of a covalent complex of nonstructural protein nsP1 with 7-methyl-GMP. Proc. Natl. Acad. Sci. USA **92:**507–511.
4. **Balistreri, G., J. Caldentey, L. Kaariainen, and T. Ahola.** 2007. Enzymatic defects of the nsP2 proteins of Semliki Forest virus temperature-sensitive mutants. J. Virol. **81:**2849–2860.
5. **Best, S. M., K. L. Morris, J. G. Shannon, S. J. Robertson, D. N. Mitzel, G. S. Park, E. Boer, J. B. Wolfinbarger, and M. E. Bloom.** 2005. Inhibition of interferon-stimulated JAK-STAT signaling by a tick-borne flavivirus and identification of NS5 as an interferon antagonist. J. Virol. **79:**12828–12839.
6. **Billecocq, A., M. Spiegel, P. Vialat, A. Kohl, F. Weber, M. Bouloy, and O. Haller.** 2004. NSs protein of Rift Valley fever virus blocks interferon production by inhibiting host gene transcription. J. Virol. **78:**9798–9806.
7. **Black, B. L., and D. S. Lyles.** 1992. Vesicular stomatitis virus matrix protein inhibits host cell-directed transcription of target genes in vivo. J. Virol. **66:**4058–4064.
8. **Bugl, H., E. B. Fauman, B. L. Staker, F. Zheng, S. R. Kushner, M. A. Saper, J. C. Bardwell, and U. Jakob.** 2000. RNA methylation under heat shock control. Mol. Cell **6:**349–360.
9. **Clark, M. E., P. M. Lieberman, A. J. Berk, and A. Dasgupta.** 1993. Direct cleavage of human TATA-binding protein by poliovirus protease 3C in vivo and in vitro. Mol. Cell. Biol. **13:**1232–1237.
10. **Cross, R. K.** 1983. Identification of a unique guanine-7-methyltransferase in Semliki Forest virus (SFV) infected cell extracts. Virology **130:**452–463.
11. **De, I., C. Fata-Hartley, S. G. Sawicki, and D. L. Sawicki.** 2003. Functional analysis of nsP3 phosphoprotein mutants of Sindbis virus. J. Virol. **77:**13106–13116.
12. **De, I., S. G. Sawicki, and D. L. Sawicki.** 1996. Sindbis virus RNA-negative mutants that fail to convert from minus-strand to plus-strand synthesis: role of the nsP2 protein. J. Virol. **70:**2706–2719.
13. **de Groot, R. J., W. R. Hardy, Y. Shirako, and J. H. Strauss.** 1990. Cleavage-site preferences of Sindbis virus polyproteins containing the non-structural proteinase. Evidence for temporal regulation of polyprotein processing in vivo. EMBO J. **9:**2631–2638.
14. **Ding, M. X., and M. J. Schlesinger.** 1989. Evidence that Sindbis virus NSP2 is an autoprotease which processes the virus nonstructural polyprotein. Virology **171:**280–284.
15. **Donelan, N. R., B. Dauber, X. Wang, C. F. Basler, T. Wolff, and A. Garcia-Sastre.** 2004. The N- and C-terminal domains of the NS1 protein of influenza B virus can independently inhibit IRF-3 and beta interferon promoter activation. J. Virol. **78:**11574–11582.
16. **Dryga, S. A., O. A. Dryga, and S. Schlesinger.** 1997. Identification of mutations in a Sindbis virus variant able to establish persistent infection in BHK cells: the importance of a mutation in the nsP2 gene. Virology **228:**74–83.
17. **Egloff, M. P., D. Benarroch, B. Selisko, J. L. Romette, and B. Canard.** 2002. An RNA cap (nucleoside-2′-*O*-)-methyltransferase in the flavivirus RNA polymerase NS5: crystal structure and functional characterization. EMBO J. **21:**2757–2768.
18. **Fata, C. L., S. G. Sawicki, and D. L. Sawicki.** 2002. Alphavirus minus-strand RNA synthesis: identification of a role for Arg183 of the nsP4 polymerase. J. Virol. **76:**8632–8640.
19. **Fata, C. L., S. G. Sawicki, and D. L. Sawicki.** 2002. Modification of Asn374 of nsP1 suppresses a Sindbis virus nsP4 minus-strand polymerase mutant. J. Virol. **76:**8641–8649.
20. **Fazakerley, J. K., A. Boyd, M. L. Mikkola, and L. Kaariainen.** 2002. A single amino acid change in the nuclear localization sequence of the nsP2 protein affects the neurovirulence of Semliki Forest virus. J. Virol. **76:**392–396.
21. **Frolov, I., E. Agapov, T. A. Hoffman, Jr., B. M. Pragai, M. Lippa, S. Schlesinger, and C. M. Rice.** 1999. Selection of RNA replicons capable of persistent noncytopathic replication in mammalian cells. J. Virol. **73:**3854–3865.
22. **Frolov, I., and S. Schlesinger.** 1994. Comparison of the effects of Sindbis virus and Sindbis virus replicons on host cell protein synthesis and cytopathogenicity in BHK cells. J. Virol. **68:**1721–1727.
23. **Frolova, E. I., R. Z. Fayzulin, S. H. Cook, D. E. Griffin, C. M. Rice, and I. Frolov.** 2002. Roles of nonstructural protein nsP2 and α/β interferons in determining the outcome of Sindbis virus infection. J. Virol. **76:**11254–11264.
24. **Garmashova, N., R. Gorchakov, E. Frolova, and I. Frolov.** 2006. Sindbis virus nonstructural protein nsP2 is cytotoxic and inhibits cellular transcription. J. Virol. **80:**5686–5696.
25. **Garmashova, N., R. Gorchakov, E. Volkova, S. Paessler, E. Frolova, and I. Frolov.** 2007. The Old World and New World alphaviruses use different virus-specific proteins for induction of transcriptional shutoff. J. Virol. **81:**2472–2484.
26. **Gomez de Cedron, M., N. Ehsani, M. L. Mikkola, J. A. Garcia, and L. Kaariainen.** 1999. RNA helicase activity of Semliki Forest virus replicase protein NSP2. FEBS Lett. **448:**19–22.
27. **Gorchakov, R., E. Frolova, and I. Frolov.** 2005. Inhibition of transcription and translation in Sindbis virus-infected cells. J. Virol. **79:**9397–9409.
28. **Griffin, D. E., and J. L. Hess.** 1986. Cells with natural killer activity in the cerebrospinal fluid of normal mice and athymic nude mice with acute Sindbis virus encephalitis. J. Immunol. **136:**1841–1845.
29. **Griffin, D. E., S. Ubol, P. Despres, T. Kimura, and A. Byrnes.** 2001. Role of antibodies in controlling alphavirus infection of neurons. Curr. Top. Microbiol. Immunol. **260:**191–200.
30. **Hahn, Y. S., E. G. Strauss, and J. H. Strauss.** 1989. Mapping of RNA-temperature-sensitive mutants of Sindbis virus: assignment of complementation groups A, B, and G to nonstructural proteins. J. Virol. **63:**3142–3150.
31. **Hardy, W. R., Y. S. Hahn, R. J. de Groot, E. G. Strauss, and J. H. Strauss.** 1990. Synthesis and processing of the nonstructural polyproteins of several temperature-sensitive mutants of Sindbis virus. Virology **177:**199–208.
32. **Hardy, W. R., and J. H. Strauss.** 1989. Processing the nonstructural polyproteins of Sindbis virus: nonstructural proteinase is in the C-terminal half of nsP2 and functions both in *cis* and in *trans*. J. Virol. **63:**4653–4664.
33. **Hardy, W. R., and J. H. Strauss.** 1988. Processing the nonstructural polyproteins of Sindbis virus: study of the kinetics in vivo by using monospecific antibodies. J. Virol. **62:**998–1007.
34. **Kaariainen, L., and M. Ranki.** 1984. Inhibition of cell functions by RNA-virus infections. Annu. Rev. Microbiol. **38:**91–109.
35. **Keranen, S., and L. Kaariainen.** 1979. Functional defects of RNA-negative temperature-sensitive mutants of Sindbis and Semliki Forest viruses. J. Virol. **32:**19–29.
36. **Kim, K. H., T. Rumenapf, E. G. Strauss, and J. H. Strauss.** 2004. Regulation of Semliki Forest virus RNA replication: a model for the control of alphavirus pathogenesis in invertebrate hosts. Virology **323:**153–163.
37. **Kuhn, R. J., Z. Hong, and J. H. Strauss.** 1990. Mutagenesis of the 3′ nontranslated region of Sindbis virus RNA. J. Virol. **64:**1465–1476.
38. **Kuhn, R. J., H. G. Niesters, Z. Hong, and J. H. Strauss.** 1991. Infectious RNA transcripts from Ross River virus cDNA clones and the construction and characterization of defined chimeras with Sindbis virus. Virology **182:**430–441.
39. **LaStarza, M. W., J. A. Lemm, and C. M. Rice.** 1994. Genetic analysis of the nsP3 region of Sindbis virus: evidence for roles in minus-strand and subgenomic RNA synthesis. J. Virol. **68:**5781–5791.
40. **Lemm, J. A., A. Bergqvist, C. M. Read, and C. M. Rice.** 1998. Template-dependent initiation of Sindbis virus RNA replication in vitro. J. Virol. **72:**6546–6553.
41. **Lemm, J. A., T. Rumenapf, E. G. Strauss, J. H. Strauss, and C. M. Rice.** 1994. Polypeptide requirements for assembly of functional Sindbis virus replication complexes: a model for the temporal regulation of minus- and plus-strand RNA synthesis. EMBO J. **13:**2925–2934.
42. **Li, G., and C. M. Rice.** 1993. The signal for translational readthrough of a UGA codon in Sindbis virus RNA involves a single cytidine residue immediately downstream of the termination codon. J. Virol. **67:**5062–5067.
43. **Li, G. P., and C. M. Rice.** 1989. Mutagenesis of the in-frame opal termination codon preceding nsP4 of Sindbis virus: studies of translational readthrough and its effect on virus replication. J. Virol. **63:**1326–1337.
44. **Lin, R. J., C. L. Liao, E. Lin, and Y. L. Lin.** 2004. Blocking of the alpha interferon-induced Jak-Stat signaling pathway by Japanese encephalitis virus infection. J. Virol. **78:**9285–9294.
45. **Mi, S., and V. Stollar.** 1991. Expression of Sindbis virus nsP1 and methyltransferase activity in *Escherichia coli*. Virology **184:**423–427.
46. **Munoz-Jordan, J. L., M. Laurent-Rolle, J. Ashour, L. Martinez-Sobrido, M. Ashok, W. I. Lipkin, and A. Garcia-Sastre.** 2005. Inhibition of α/β interferon signaling by the NS4B protein of flaviviruses. J. Virol. **79:**8004–8013.
47. **Munoz-Jordan, J. L., G. G. Sanchez-Burgos, M. Laurent-Rolle, and A. Garcia-Sastre.** 2003. Inhibition of interferon signaling by dengue virus. Proc. Natl. Acad. Sci. USA **100:**14333–14338.
48. **Niesters, H. G., and J. H. Strauss.** 1990. Mutagenesis of the conserved 51-nucleotide region of Sindbis virus. J. Virol. **64:**1639–1647.
49. **Owen, K. E., and R. J. Kuhn.** 1996. Identification of a region in the Sindbis virus nucleocapsid protein that is involved in specificity of RNA encapsidation. J. Virol. **70:**2757–2763.
50. **Park, G. S., K. L. Morris, R. G. Hallett, M. E. Bloom, and S. M. Best.** 2007. Identification of residues critical for the interferon antagonist function of Langat virus NS5 reveals a role for the RNA-dependent RNA polymerase domain. J. Virol. **81:**6936–6946.
51. **Peranen, J., M. Rikkonen, P. Liljestrom, and L. Kaariainen.** 1990. Nuclear localization of Semliki Forest virus-specific nonstructural protein nsP2. J. Virol. **64:**1888–1896.
52. **Peranen, J., K. Takkinen, N. Kalkkinen, and L. Kaariainen.** 1988. Semliki Forest virus-specific non-structural protein nsP3 is a phosphoprotein. J. Gen. Virol. **69:**2165–2178.
53. **Perri, S., D. A. Driver, J. P. Gardner, S. Sherrill, B. A. Belli, T. W. Dubensky, Jr., and J. M. Polo.** 2000. Replicon vectors derived from Sindbis virus and

Semliki Forest virus that establish persistent replication in host cells. J. Virol. **74:**9802–9807.
54. **Reyes, G. R.** 2002. The nonstructural NS5A protein of hepatitis C virus: an expanding, multifunctional role in enhancing hepatitis C virus pathogenesis. J. Biomed. Sci. **9:**187–197.
55. **Rikkonen, M.** 1996. Functional significance of the nuclear-targeting and NTP-binding motifs of Semliki Forest virus nonstructural protein nsP2. Virology **218:**352–361.
56. **Rikkonen, M., J. Peranen, and L. Kaariainen.** 1994. ATPase and GTPase activities associated with Semliki Forest virus nonstructural protein nsP2. J. Virol. **68:**5804–5810.
57. **Rikkonen, M., J. Peranen, and L. Kaariainen.** 1992. Nuclear and nucleolar targeting signals of Semliki Forest virus nonstructural protein nsP2. Virology **189:**462–473.
58. **Rikkonen, M., J. Peranen, and L. Kaariainen.** 1994. Nuclear targeting of Semliki Forest virus nsP2. Arch. Virol. Suppl. **9:**369–377.
59. **Russo, A. T., M. A. White, and S. J. Watowich.** 2006. The crystal structure of the Venezuelan equine encephalitis alphavirus nsP2 protease. Structure **14:** 1449–1458.
60. **Salonen, A., L. Vasiljeva, A. Merits, J. Magden, E. Jokitalo, and L. Kaariainen.** 2003. Properly folded nonstructural polyprotein directs the Semliki Forest virus replication complex to the endosomal compartment. J. Virol. **77:**1691–1702.
61. **Sawicki, D. L., S. Perri, J. M. Polo, and S. G. Sawicki.** 2006. Role for nsP2 proteins in the cessation of alphavirus minus-strand synthesis by host cells. J. Virol. **80:**360–371.
62. **Sawicki, D. L., and S. G. Sawicki.** 1985. Functional analysis of the A complementation group mutants of Sindbis HR virus. Virology **144:**20–34.
63. **Sawicki, D. L., R. H. Silverman, B. R. Williams, and S. G. Sawicki.** 2003. Alphavirus minus-strand synthesis and persistence in mouse embryo fibroblasts derived from mice lacking RNase L and protein kinase R. J. Virol. **77:**1801–1811.
64. **Sawicki, S. G., D. L. Sawicki, L. Kaariainen, and S. Keranen.** 1981. A Sindbis virus mutant temperature-sensitive in the regulation of minus-strand RNA synthesis. Virology **115:**161–172.
65. **Shirako, Y., and J. H. Strauss.** 1994. Regulation of Sindbis virus RNA replication: uncleaved P123 and nsP4 function in minus-strand RNA synthesis, whereas cleaved products from P123 are required for efficient plus-strand RNA synthesis. J. Virol. **68:**1874–1885.
66. **Shirako, Y., and J. H. Strauss.** 1998. Requirement for an aromatic amino acid or histidine at the N terminus of Sindbis virus RNA polymerase. J. Virol. **72:**2310–2315.
67. **Simmons, D. T., and J. H. Strauss.** 1972. Replication of Sindbis virus. II. Multiple forms of double-stranded RNA isolated from infected cells. J. Mol. Biol. **71:**615–631.
68. **Strauss, E. G., C. M. Rice, and J. H. Strauss.** 1984. Complete nucleotide sequence of the genomic RNA of Sindbis virus. Virology **133:**92–110.
69. **Strauss, E. G., C. M. Rice, and J. H. Strauss.** 1983. Sequence coding for the alphavirus nonstructural proteins is interrupted by an opal termination codon. Proc. Natl. Acad. Sci. USA **80:**5271–5275.
70. **Strauss, J. H., and E. G. Strauss.** 1994. The alphaviruses: gene expression, replication, and evolution. Microbiol. Rev. **58:**491–562.
71. **Suopanki, J., D. L. Sawicki, S. G. Sawicki, and L. Kaariainen.** 1998. Regulation of alphavirus 26S mRNA transcription by replicase component nsP2. J. Gen. Virol. **79:**309–319.
72. **Talon, J., C. M. Horvath, R. Polley, C. F. Basler, T. Muster, P. Palese, and A. Garcia-Sastre.** 2000. Activation of interferon regulatory factor 3 is inhibited by the influenza A virus NS1 protein. J. Virol. **74:**7989–7996.
73. **Tomar, S., R. W. Hardy, J. L. Smith, and R. J. Kuhn.** 2006. Catalytic core of alphavirus nonstructural protein nsP4 possesses terminal adenylyltransferase activity. J. Virol. **80:**9962–9969.
74. **Vasiljeva, L., A. Merits, P. Auvinen, and L. Kaariainen.** 2000. Identification of a novel function of the alphavirus capping apparatus. RNA 5′-triphosphatase activity of Nsp2. J. Biol. Chem. **275:**17281–17287.
75. **Wang, H. L., J. O'Rear, and V. Stollar.** 1996. Mutagenesis of the Sindbis virus nsP1 protein: effects on methyltransferase activity and viral infectivity. Virology **217:**527–531.
76. **Wang, Y. F., S. G. Sawicki, and D. L. Sawicki.** 1994. Alphavirus nsP3 functions to form replication complexes transcribing negative-strand RNA. J. Virol. **68:**6466–6475.
77. **Wang, Y. F., S. G. Sawicki, and D. L. Sawicki.** 1991. Sindbis virus nsP1 functions in negative-strand RNA synthesis. J. Virol. **65:**985–988.
78. **Weaver, S. C., and A. D. Barrett.** 2004. Transmission cycles, host range, evolution and emergence of arboviral disease. Nat.Rev. Microbiol. **2:**789–801.
79. **Yalamanchili, P., R. Banerjee, and A. Dasgupta.** 1997. Poliovirus-encoded protease 2APro cleaves the TATA-binding protein but does not inhibit host cell RNA polymerase II transcription in vitro. J. Virol. **71:**6881–6886.